JOURNAL OF Applied Polymer SCIENCE

"Pore/Bead" Membrane for Rechargeable Lithium Ion Batteries

Yuezeng Su,[1] Feng Shan,[2] Zhiming Li,[2] Xinling Wang[2]

[1]School of Aeronautics and Astronautics, Shanghai Jiao Tong University, Shanghai 200240, China

[2]School of Chemistry & Chemical Engineering, State Key Laboratory of Metal Matrix Composites, Shanghai Jiaotong University, Shanghai 200240, China

Correspondence to: X. Wang (E-mail: xlwang@sjtu.edu.cn)

ABSTRACT: A special "pore/bead" membrane was prepared with a mesoporous inorganic filler (MCM-41) and a P(VDF-HFP) binder. The special "pore/bead" structure of the MCM-41 filler not only enhanced the puncture strength of the membrane but also improved its ionic conductivity. The puncture strength of the dried "pore/bead" membrane (MCM-41 : P(VDF-HFP) = 1 : 1.5) was 18 N, and showed a slight decrease (16 N) after the membrane was wetted by liquid electrolyte. Additionally, the composite membrane showed excellent thermal dimensional stability. The composite membrane could be activated by adding 1*M* $LiClO_4$-EC/DMC (1 : 1 by volume). The activated membrane displayed a high ionic conductivity about 3.4×10^{-3} S cm^{-1} at room temperature. Its electrochemical stability window was up to 5.3 V vs. Li/Li^+, indicating that it was very suitable for lithium-ion battery application. The battery assembled using the composite electrolyte also showed reasonably good high-rate performance. The approach of preparing a "pore/bead" membrane provides a new avenue for improving both the conductivity and the mechanical strength of polymer electrolytes for lithium batteries. © 2012 Wiley Periodicals, Inc. J. Appl. Polym. Sci. 000: 000–000, 2012

KEYWORDS: 'pore/bead'; membrane; lithium-ion battery; safety

Received 16 August 2011; accepted 29 February 2012; published online 00 Month 2012

DOI: 10.1002/app.37625

INTRODUCTION

Commercialized lithium-ion batteries, consisting of graphite-based anodes, $LiCoO_2$-based cathodes, and organic solvent electrolytes, have several advantages, such as a high operating voltage, a high energy density and relatively good cycle durability. However, the use of a flammable and easily leaking liquid electrolyte is unavoidable in the present lithium ion batteries. In the past few years, rechargeable lithium ion batteries using polymer electrolyte separators have been known as preferred power source for various applications because of their high energy density, long cycle life, and memory-free effect.[1,2] The properties of polymer electrolyte significantly affect the performance and safety of lithium ion battery. For Li-ion batteries to have good rate capability, the gelled polymer electrolyte (GPE) is required to imbibe a significant amount of liquid. However, this adversely affects the mechanical strength of the GPE separator. The safety requirement is a top priority for rechargeable lithium ion batteries, especially those used in hybrid electric vehicles and power tools.

GPEs that meet the conductivity requirement for general-purpose batteries (10^{-3} S/cm at room temperature) typically have low inherent dimensional stability and mechanical strength due to the large amount of liquid electrolyte absorbed. In the past 10–20 years, various efforts have therefore been put on developing processable GPEs with good conductivity, mechanical strength, and thermal stability. For example, ceramic fillers, such as TiO_2, SiO_2, Al_2O_3, MgO, ZrO_2, clay, and, CNT are doped in GPEs.[3-8] Another method is to use dual phase polymer electrolytes which are composed of one phase adapted to absorb liquid electrolyte and the other phase which is stronger, tougher, and substantially inert against liquid electrolytes.[9-11] The absorbing phase functions as a tunnel for ion transport and the inert phase can support the electrolyte membrane. Cross-linking approach has also been applied to enhance the dimensional stability of GPEs.[12] Despite the significant improvement achieved, the presence of liquid electrolyte in GPEs inevitably brings side-effects to their dimensional stability and mechanical strength. These disadvantages limit their commercial application especially in large-sized batteries.

In porous polymer electrolytes, high porosity and interconnected pore structure are necessary to enable the membrane with high ionic conductivity.[13-16] However, there are many locally "open" areas in porous polymer electrolytes which may

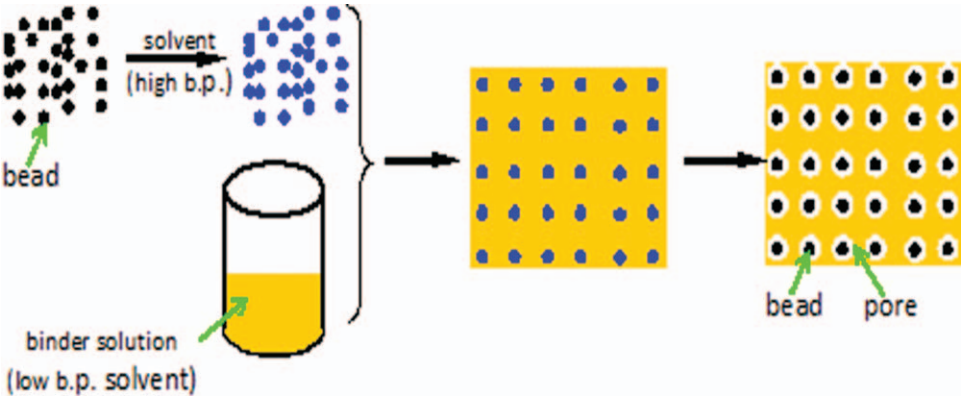

Scheme 1. The process of preparing "pore/bead" membrane. [Color figure can be viewed in the online issue, which is available at wileyonlinelibrary.com.]

result in short-circuit through the membrane. Furthermore, it will increase the difficulty on battery assembly due to their low puncture strength. To solve these problems, Degussa developed a series of Separion (trademark) membrane by coating a porous ceramic layer onto both sides of the non-woven PET substrate.[17] Remarkable improvements on the battery safety have been demonstrated from using these membranes on a series of abuse tests. However, the cost is very high due to their complicated manufacturing process.

In this report, we firstly reported a facile approach to the preparation of "pore/bead" membranes (illustrated in Scheme 1). The bead had three functions: (1) forming pore; (2) soaking liquid electrolyte; (3) improving mechanical strength. In this work, mesoporous silica was chosen as the bead and poly(vinylidene fluoride-hexafluoropropylene) [P(VDF-HFP)] as the binder. The preparation and characterization of the composite membrane were discussed. The prepared membranes could be activated by using 1*M* $LiClO_4$-EC/DMC (1 : 1 by volume) electrolyte. The electrochemical properties of the composite electrolyte were also studied. Preliminary results showed that the gel polymer electrolyte could be used for scale-up lithium ion battery. The GPEs prepared by using mesoporous filler and binder provided a new method for further improving both the conductivity and mechanical strength of GPEs.

EXPERIMENTAL

Materials

P(VDF-HFP) (Kynar Flex 2751) was purchased from Elf Atochem. Its melt volume-flow rate is 1.9 cm^3/10 min, and its density is 1.78 kg/m^3. Mesoporous silica (MCM-41) was kindly provided by Toray Corporation. The other reagents were local commercial products and used without further purification.

Preparation of "Pore/Bead" Membrane

The Scheme 1 showed the preparation of "pore/bead" membrane. MCM-41 was dispersed in *N*-methyl-2-pyrrolidone (NMP) (MCM-41 : NMP = 1 : 4 in weight ratio), and followed by adding a certain amount of P(VDF-HFP) solution (15 wt %, THF as solvent) into the mixture prepared earlier by stirring. The obtained homogenized suspension was cast on Teflon plate. When the THF was evaporated in a dry atmosphere and the membrane took shape, the resulting membrane was heated in a vacuum oven at 100°C to remove NMP and form the "pore/bead" membrane ($\sim$ 40 μm in thickness).

Field Emission Scanning Electron Microscope Analysis

Field emission scanning electron microscope (FESEM) images of the membrane surface were observed on JEOL JSM 7401F with gold-sputtered-coated films at an activation voltage of 5 kV.

Brunauer–Emmett–Teller Analysis

The pore parameters and surface area of the samples were measured using at 77 K using Micromeritics ASAP 2010 M+C nitrogen adsorption apparatus. Prior to the measurement, the samples were degassed at a temperature of 120°C for approximately 4 hr. The nitrogen adsorption/desorption data were recorded at 77 K. The specific surface area was calculated using the Brunauer–Emmett–Teller (BET) equation. The BET method is widely used in surface science for the calculation of surface areas of solids by physical adsorption of gas molecules. The BET equation is as follows:

$$\frac{1}{v[(P_0/P)-1]} = \frac{c-1}{v_m c}\left(\frac{P}{P_0}\right) + \frac{1}{v_m c} \quad (1)$$

P and P_0 are the equilibrium and the saturation pressure of adsorbates at the temperature of adsorption, v is the adsorbed gas quantity, and v_m is the monolayer adsorbed gas quantity. c is the BET constant. The pore size distribution was determined by the Barrett–Joyner–Halenda (BJH) method.

Puncture Strength Measurement

The puncture strength of the membrane was determined by using a needle (a 0.8-mm-diameter ball) to penetrate the membrane. Dynamometer (TA-108S) was used to measure the force with a test speed of 1 mm/s.

Thermal Shrinkage Measurement

The thermal shrinkage was determined as follows:

$$\text{thermalshrinkage}(\%) = (D_0 - D)/D_0 \quad (2)$$

where D_0 and D represented the diameter of the membrane before and after heat, respectively.

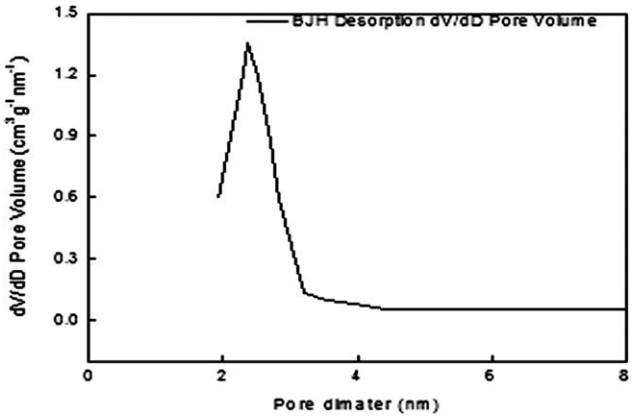

Figure 1. BJH pore size distribution of MCM-41.

Liquid Uptake Measurement

The uptake amount of liquid electrolyte was determined as follows:

$$\text{uptake}(\%) = (M - M_0)/M_0 \tag{3}$$

where M_0 and M represented the weight of the samples before and after immersion in liquid electrolyte, respectively.

Ionic Conductivity Measurement

The composite electrolyte was sandwiched between two stainless steel blocking electrodes. The ionic conductivities of the polymer electrolytes were obtained from the bulk resistance (R_b) measured by AC complex impedance analysis using a Solatron 1287 frequency response analyzer over a frequency range of 10 Hz−1 MHz at amplitude of 5 mV. The ionic conductivity (σ) of polymer electrolyte was determined as follows:

$$\sigma = t/(R_b\text{A}) \tag{4}$$

where t is the thickness of the membrane and A is the surface area of the membrane.

Electrochemical Stability Window Measurement

The electrochemical stability of the composite electrolyte (immersing the dry "pore/bead" membrane into a 1.0*M* $LiClO_4$-EC/DMC (1 : 1 by volume) solution at room temperature for 1 hr) was evaluated by sweep voltammetry at 25°C. Discs of the composite electrolyte were sandwiched between a lithium metal counter electrode and a stainless steel working electrode (having a 10 mm diameter) and, then, placed inside a Teflon cell holder. A sweeping voltage (1 mV/s) was applied to the cell starting from the open circuit voltage. When the composite electrolyte decomposition took place a large current passed through the cell. The decomposition voltage was evaluated as the onset of the current increase on the voltage/current plots. The measurement was carried out by using a Solartron Electrochemical Interface 1287.

Electrochemical Property Measurement

Anode was prepared by coating the slurry of mesocarbon microbead (90%), PVDF binder (7%), and acetylene black (3%) onto a copper foil with a doctor blade. The cathode slurry containing the same PVDF binder (6%) and acetylene black (4%) along with $LiCoO_2$ (90%) cathode material was cast on aluminum foil. The thickness of the electrodes ranged from 60 to

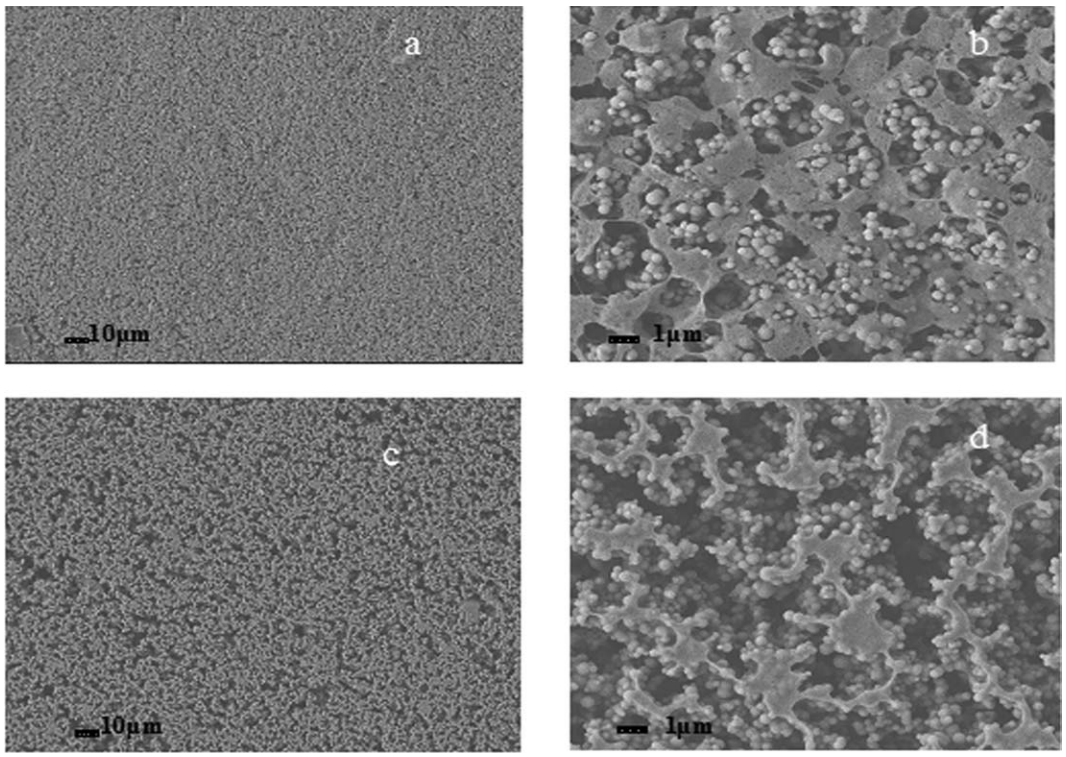

Figure 2. FESEM images of the "pore/bead" membranes.

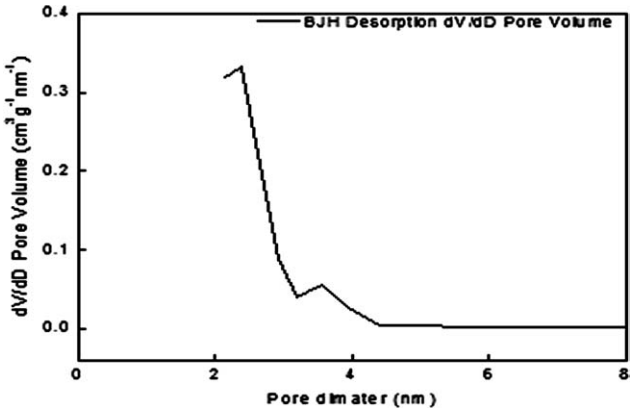

Figure 3. BJH pore size distribution of the "pore/bead" membrane [MCM-41 : P(VDF-HFP) =1 : 1.5).

80 μm. The coated electrodes were dried under vacuum at 120°C for 8 hr. The coin cells were assembled by sandwiching the composite electrolyte between anode and cathode in an argon-filled glove box. Charge–discharge performance of the coin cells was characterized on a battery testing system (RF-T, Roofer Group Company, China) between 2.5 and 4.2 V. In rate property test, the cell was charged at C/10 rate to 4.2 V and then discharged at different current densities to 2.5 V.

RESULTS AND DISCUSSION

Morphology of "Pore/Bead" Membrane

Mesoporous material played an important role on enhancement of ionic conductivity by caging ion conductor into its interconnective ordered channels. MCM-41 was a kind of mesoporous silica with BET-specific surface area of 1030 m^2 g^{-1} and an average diameter of 2.6 nm (as shown in Figure 1). When NMP was added into MCM-41, the inter-connective channels in MCM-41 would be filled by NMP. It could decrease the binder solution penetration, thus lowered the possibility of blocking ion channels. On the other hand, during the process of heating the resulting membrane (after removing THF) in a vacuum oven at 100°C, large quantity pores were formed after the evaporation of NMP solvent, resulting in the desired "pore/bead" structure. These were confirmed in Figure 2(b). The porosity increased with the increase of MCM-41. However, when the weight ratio of MCM-41 and P(VDF-HFP) reached 1, the binder became the dispersed phase [Figure 2(d)] and the obtained membrane was very fragile.

The BJH pore size distribution of the prepared membrane [MCM-41 : P(VDF-HFP) =1 : 1.5] was displayed in Figure 3. Besides the pore size of MCM-41, a new peak in 3.6 nm appeared. It probably represented a new pore forming at the process of removing NMP. Meanwhile, there were many large pores which could not be measured in this method. The BET-specific surface area of the as prepared membrane was 466 m^2 g^{-1}, and the large specific surface area was very helpful to absorb liquid electrolyte.

Mechanical Properties of "Pore/Bead" Membrane

The polymer electrolyte used in battery required high puncture strength to avoid penetration of electrode material through it. If articulate material from the electrodes penetrated the electrolyte, it would result in an electrical short circuit. The puncture strength of "pore/bead" membrane [MCM-41 : P(VDF-HFP) =1 : 1.5] was 18 N, which was higher than commercialized Celgard 2500 separator (14 N). Only a slight decrease in puncture strength (16 N) took place when the membrane absorbed liquid electrolyte. The puncture resistance was high enough for the GPE membrane to be used as separators in Li-ion batteries. These results demonstrated MCM-41 in the pore provided exceptional puncture strength.

Thermal shrinkage or melting was very dangerous in battery, because it would result in physical contact between anode and cathode. So, membrane thermal shrinkage was a key index to lithium ion battery, especially for large-size lithium ion battery.[2,18] When Celgard 2500 separator was treated at 90°C for 60 min, the shrinkage was 5%, but it shrank as much as 10% when exposed at 120°C only for 10 min. Nevertheless, a negligible shrinkage was found in the "pore/bead" membrane at 120°C even for 60 min. The outstanding dimensional stability was very helpful in improving battery safety.

Liquid Uptake and Ionic Conductivity

Figure 4 showed the uptake of liquid electrolyte [$LiClO_4$-EC/DMC (1 : 1 by volume)] for "pore/bead" membrane [MCM-41 : P(VDF-HFP) = 1 : 1.5] as the function of soaking time. In the "pore/bead" membrane, the liquid electrolyte uptake process was very fast and the maximum amount of electrolyte penetrated into the membrane within a few seconds. These were due to the facts that high specific surface area and high hydrophilicity of MCM-41 bead exhibited excellent wettability with liquid electrolyte.[19] Meanwhile, both the pore and the bead in the membrane could soak liquid electrolyte, the maximum liquid uptake reached as high as 150%.

Figure 5 showed the variable temperature conductivity of activated "pore/bead" membrane [MCM-41 : P(VDF-HFP) =1 : 1.5]

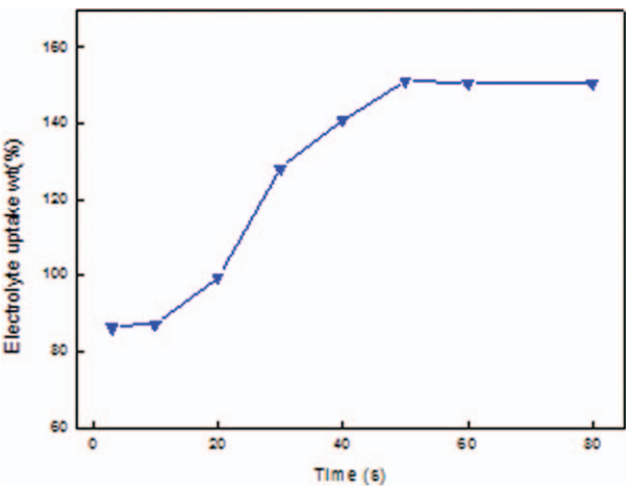

Figure 4. The liquid electrolyte uptake of the "pore/bead" membrane [MCM-41 : P(VDF-HFP) =1 : 1.5] as the function soaking time, 25°C. [Color figure can be viewed in the online issue, which is available at wileyonlinelibrary.com.]

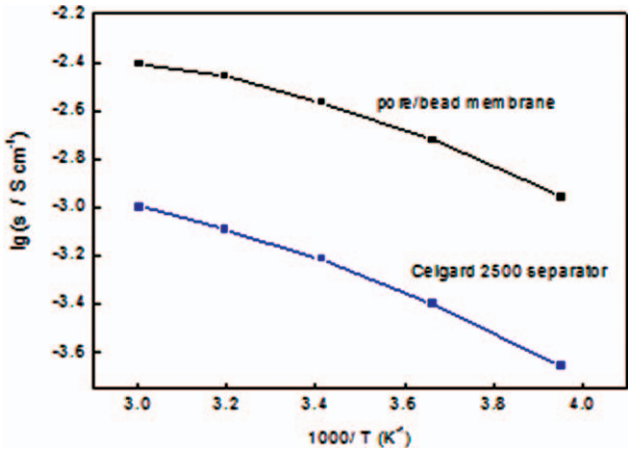

Figure 5. Arrhenius plots of ionic conductivity for the "pore/bead" membrane [MCM-41 : P(VDF-HFP) =1 : 1.5] and Celgard 2500 separator containing1*M* $LiClO_4$/EC-DMC (1 : 1 vol %). [Color figure can be viewed in the online issue, which is available at wileyonlinelibrary.com.]

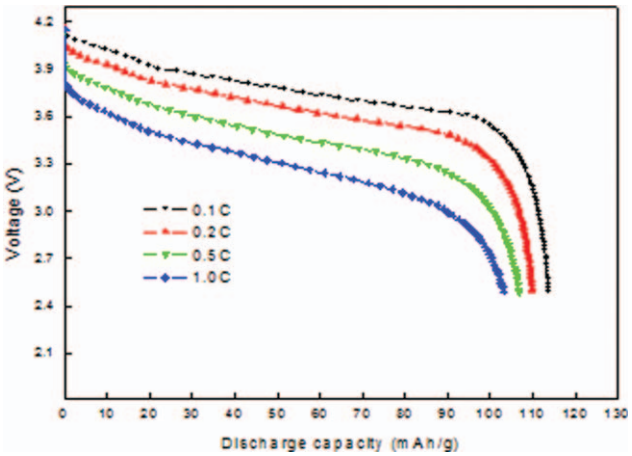

Figure 7. Discharge capacities of $LiCoO_2$-MCMB coin cells containing activated "pore/bead" membrane [MCM-41 : P(VDF-HFP) = 1 : 1.5] at different C-rates. 2.5–4.2 V, 25°C. [Color figure can be viewed in the online issue, which is available at wileyonlinelibrary.com.]

and Celgard 2500 membrane. The ionic conductivity increased with increasing temperature. The room-temperature ionic conductivity of "pore/bead" membrane was 3.4 × 10^{-3} S cm^{-1}. Even at −20°C, the conductivity was still greater than 1.0 × 10^{-3} S cm^{-1}. The ionic conductivity was high enough for practical applications in lithium ion battery. The room-temperature ionic conductivity of Celgard 2500 membrane was closed to 1.0 × 10^{-3} S cm^{-1} and the low temperature ionic conductivity (−20°C) decreased to 2.6 × 10^{-4} S cm^{-1}. The high conductivity of "pore/bead" membrane was probably related to the high liquid uptake and inter-connective ion channels both in the pore and in the bead. On the other hand, the filler/salt interaction played an important role in enhancement of ionic conductivity.[20,21]

Electrochemical Properties

For determining the electrochemical stability window of the "pore/bead" composite electrolyte, a linear sweep voltammetry experiment was performed in the potential range of 0.0–6.0 V (versus Li/Li^+) with a scan rate of 5 mV s^{-1}. Figure 6 showed the electrochemical stability window of the composite electrolyte

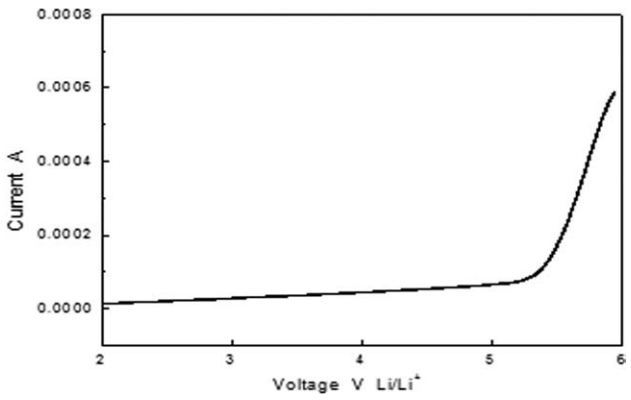

Figure 6. Electrochemical stability window of the composite electrolyte [MCM-41 : P(VDF-HFP) =1 : 1.5) by linear sweep voltammogram.

[MCM-41 : P(VDF-HFP) = 1 : 1.5]. The onset current flow was associated with the decomposition voltage of the electrolyte. It was found that the oxidation occurred (current flow increased rapidly) at potentials higher than 5.3 V. So, the composite electrolyte was very suitable for lithium-ion battery applications.

To evaluate the electrochemical performance of lithium ion battery using the composite electrolyte, MCMB/composite electrolyte/$LiCoO_2$ battery was assembled. The discharge curves of the battery at various discharging rate were shown in Figure 7. The figure revealed that the battery at 0.1C rate could achieve a good capacity of 113.9 mA h g^{-1}. With the increase of current rate, both the voltage and the capacity were found to be gradually decreased. At 1.0 C discharge rate, the capacity decreased to 103.2 mA h g^{-1}. The decline in capacity might come from the lost of interfacial contact between electrodes and the composite electrolyte upon cycling, which gradually increased the internal resist of the cell. Further study about the capacity decline was under way. The voltage drops in passing from the charge to discharge increased with the discharge rate, reflecting a large polarization that reduced the discharge capacity. However, the tested battery still retained ∼ 90% of discharge capacity at 1.0 C rate, as compared with that at 0.1 C rate.

CONCLUSIONS

The introduction of pore and bead into a composite membrane was a novel approach to achieve excellent comprehensive properties electrolyte. The special "pore/bead" structure made from MCM-41 bead not only enhanced membrane puncture strength but also improved its ionic conductivity. The "pore/bead" membrane showed higher puncture strength, excellent thermal dimensional stability, and high ionic conductivity. Its electrochemical stability window was stable up to 5.3 V, which was very suitable for lithium-ion battery application. The battery assembled by the composite electrolyte showed reasonably good high-rate performance. Preliminary results showed that it was promising as polymer electrolytes for scale-up lithium ion battery.

ACKNOWLEDGMENTS

This project is supported by the Shanghai Leading Academic Discipline Project of Shanghai Municipal Education Commission.

REFERENCES

1. Xue, J. S.; Wise, R. D.; Zhang, X. L.; Manna, M. E.; Lu, Y. X.; Ducharme, G.; Cuellar, E. A.; *J. Power Sources* **1999,** *80*, 119.
2. Choi, Y. S.; Bae, Y. C.; Sun, Y. K. *J. Appl. Polym. Sci.* **2005,** *98*, 2314.
3. Low, S. P.; Ahmad, A.; Hamzah, H.; Rahman, M. Y. A. *J. Solid State Electrochem.* **2011,** *15*, 2611.
4. Sundaram, N. T. K.; Subramania, A. *Electrochim. Acta* **2007,** *52*, 4987.
5. Suthanthiraraj, S. A.; Kumar, R.; Paul, B. J.; Mathew, V. *J. Solid State Electrochem.* **2011,** *15*, 561.
6. Suthanthiraraj, S. A.; Kumar, R.; Paul, B. J. *Trans. Indian Inst. Metals* **2011,** *64*, 155.
7. Ibrahim, S.; Ali, S. A. H.; Mohamed, N. S. *Adv. Mater. Res.*, **2010,** *93–94*, 489.
8. Deka, M.; Kumar, A. *J. Power Sources* **2011,** *196*, 1358.
9. Ibrahim, S.; Johan, M. R. *Int. J. Electrochem. Sci.* **2011,** *6*, 5565.
10. Li, Z. M.; Shan, F.; Wei, J. G.; Yang, J.; Li, X. S.; Wang, X. L.; *J. Solid State Electrochem.* **2008,** *12*, 1629.
11. Tian, Z.; Pu, W. H.; He, X. M.; Wan, C. R.; Jiang, C. Y. *Electrochim. Acta* **2007,** *52*, 3199.
12. Hou, X. P.; Siow, K. S. *J. Solid State Electrochem.* **2001,** *5*, 293.
13. Unal, B.; Klein, R. J.; Yocca, K. R.; Hedden, R. C. *Polymer* **2007,** *48*, 6077.
14. Cao, J. H.; Zhu, B. K.; Xu, Y. Y. *J. Membr. Sci.* **2006,** *281*, 446.
15. Kim, K. M.; Park, N. G.; Ryu, K. S.; Chang, S. H. *J. Appl. Polym. Sci.* **2006,** *102*, 140.
16. He, X. M.; Shi, Q.; Zhou, X.; Wan, C. R.; Jiang, C. Y. *Electrochim. Acta* **2005,** *51*, 1069.
17. Jiang, Y. X.; Chen, Z. F.; Zhuang, Q. C.; Xu, J. M.; Dong, Q. F.; Huang, L.; Sun, S. G. *J. Power Sources* **2006,** *160*, 1320.
18. Duelmen, V. H.; Rhede, C. H.; Nottuln, G. H.; Brugg, P. N.; Wurenlingen, J. V. US Patent 20060078791 (**2006**).
19. Kritzer, P. *J. Power Sources* **2006,** *161*, 1335.
20. Kimura, T.; Sugahara, Y.; Kuroda, K. *Microporous Mesoporous Mater* **1998,** *22*, 115.
21. Tominaga, Y.; Igawa, S.; Asai, S.; Sumita, M. *Electrochimica Acta* **2005,** *50*, 3949.